Modelling and Performance Assessment of a Standalone Solar Water Pumping System for Agricultural Applications

Udyan Kumar Jha[1, 2], Rahul Gupta[1], Neelu Nagpal[2*]

[1]Maharaja Agrasen University, University, Baddi, Himachal Pradesh, India.
[2]Maharaja Agrasen Institute of Technology, Delhi, India

Abstract

This paper investigates the performance of an advanced standalone solar water pumping sys- tem (SSWPS) model intended for off-grid agricultural applications. The model comprises a photovoltaic (PV) array, an Incremental Conductance (INC)-based Maximum Power Point Tracking (MPPT) controller, a high-gain LUO DC-DC converter, and a three-phase Brush- less Direct Current (BLDC) motor directly coupled to a centrifugal pump. With the primary objective for an optimal energy harvesting and reliable water pumping under fluctuating so- lar irradiance, an MPPT algorithm dynamically modulates the duty cycle of the proposed LUO converter. Simulation tests at varying duty cycles of the converter represent the full range of operational irradiance conditions to indicate the effective voltage regulation across varying inputs to maintain a stable output even when the input voltage drops significantly. The system achieves a maximum efficiency of 94.78% on a duty cycle of 0.75, where the con- verter's superlift capability drives the motor at a stable 2065 rpm and 5.0 Nm with minimal current ripple. Furthermore, the economic assessment of the system reveals a Levelized Cost of Energy (LCOE) of 0.351/kWh. From an environmental perspective, the analysis high- lights substantial annual carbon savings of 1,611 kg of CO_2, and a carbon payback period of 1.6 years. A comparative analysis with alternative work justifies the efficacy of the proposed model design. This integrated methodology, which combines detailed performance modeling with key economic and environmental metrics, offers a holistic framework for designing and implementing renewable energy water pumping solutions.

Keywords: BLDC Motor; Carbon Savings; LUO DC-DC Converter; Renewable Energy; System Optimization; Water Pumping Systems

1 Introduction

With growing global water and energy needs, solar-powered water pumping systems are be- coming game-changing technologies, especially for off-grid and agricultural applications [1, 2]. This applies particularly to regions where the demand for water directly correlates with the availability of solar radiation [3]. The worldwide solar water pump market, which was around USD 1.5 billion in 2024, is expected to grow more than two times to around USD 3 billion by 2029, at a CAGR of 9–13% [2]. Favorable government policies and falling solar panel prices in Asia Pacific and India are major drivers, and submersible solar pumps have more than 50% market share as they can pump from deeper water levels. The SSWPS traditionally has utilized direct drive (DC) or alternating current (AC) motors. The utilization of BLDC mo- tors in the system design provides some major benefits, including higher efficiency, improved torque-to-weight ratio, reduced maintenance requirements, and compatibility with digital con- trol systems [6]. All these considerations promoted grown interest in solar pumping systems utilizing BLDC motors, particularly with matched power electronic circuits [4, 5]. Further, [4] has demonstrated that when battery storage is integrated into solar water pumping systems, it mitigates the effects of solar intermittency, thereby extending daily operational hours by preventing disruptive stop/start cycles. However, this approach introduces notable disadvan- tages, including a higher initial capital cost and a reduction in end-to-end system efficiency. A systematic procedure is required for the complete design of an SSPWS that can compute the system's output, specifically the hourly flow rate of the pump, based on various inputs. In this regard, a case study by [7] proposed an algorithm for hourly water flow rates, taking into account hourly global solar radiation, ambient temperature, and wind speed as inputs. It also incorporates regional characteristics and PV system parameters. The appropriate selection of PV modules is crucial to reduce installation, maintenance, and overall system cost [3, 8]. A key feature of maximizing solar energy utilization is the use of the MPPT algorithm. Of the MPPT techniques available, Incremental Conductance (INC) and its adaptive variants are noted for their improved tracking speed and

accuracy under changing irradiance conditions [23]. Recent works have boosted the performance of MPPT by the use of artificial neural network (ANN) based or hybrid techniques in order to deal with practical situations such as partial shading or transient cloud cover [9, 10, 11, 12]. The study of [13] has focused on the high-level design using HOMER simulation tools to determine the optimal sizing and combi- nation of components such as PV panels, wind turbines, and batteries. While these studies successfully model overall energy production, they frequently neglect to investigate the inherent torque ripples in the BLDC motor drives that are commonly used, a factor that directly causes mechanical stress and reduces the system's long-term reliability. Another work of SSP- WPS [14] has designed the model using PVSyst and SoSiT simulation tools, and estimated the unit (kWh) cost of the proposed pumping system. The economic models of this system often assume idealized energy capture, failing to account for the suboptimal performance of conventional MPPT algorithms under the rapidly fluctuating solar irradiance typical of off- grid sites [15]. A case study by [16] focused on the life cycle assessment (LCA) of complete SSWPS. It analyzed the different materials used, applying the methodology outlined in ISO 14040 and 14044 standards [17]. Based on their LCA, they proposed a common reference benchmark to calculate the net CO2 emissions from the system, specifically per unit volume of water pumped to a unit discharge height. In solar water pumping systems, CO_2 emissions are consistently reported as lower [18, 8]. We have considered the literature specifically on SSWPS to extract the research gaps.

Table 1: Summary of Literature Review

S. No.	**Ref. Used**	**System/Technical Analysis/Focus**	**Economic Analysis**	**Reliability Analysis**	**CO_2 Emission**
1	[3]	Explored relationship between motor voltage and pump flow rate.	√	×	×
2	[7], [28]	Developed method for computing hourly pump flow rate & analyzed pump & motor without component-wise detail.	√	×	×
3	[16]	Analysis of centrifugal multistage pump with VFD AC drive.	√	√	√
4	[14]	Focused on technical analysis centrifugal multistage pumps	×	×	×
5	[12]	Investigated various types of Incremental Conductance MPPT controllers.	√	×	×
7	[8]	Comprehensive system design and analysis.	√	×	×
8	**Proposed**	**Design a SSPWS that investigates component-wise & system performance evaluation under diverse solar and duty cycle conditions.**	√	√	√

As presented in Table 1, it is observed that existing research on this topic often focuses on overall feasibility, neglecting the detailed analysis of component-level inefficiencies that reduce power output and system reliability. These gaps are discussed as below.

- The majority of existing research presents a fragmented analysis, often evaluating technical performance in isolation from long-term reliability, economic viability, or environmental impact. This siloed approach prevents a holistic understanding of system feasibility and fails to provide stakeholders with a single, integrated framework for making well-rounded decisions.
- This research addresses this gap by investigating a specific power electronics interface de- signed to mitigate performance losses, such as current and torque ripple, thereby maximiz ing the efficiency of the core electrical components and improving the system's practical performance in the field.

- While many studies identify an optimal operating point, they often lack a deep investigation into the critical trade-offs and failure modes associated with suboptimal operation. There is a specific gap in quantifying how component-level efficiencies are directly correlated with the power converter's duty cycle, which is essential for defining safe and reliable operational boundaries.
- The central conflict between the high upfront cost and the positive environmental impact of solar pumping technology is often discussed qualitatively. However, there is a notable absence of studies that provide a concrete, data-driven quantification of this trade-off by presenting metrics like Levelized Cost of Energy (LCOE) and annual carbon savings side- by-side.
- Reliability and lifetime analyses for SSPWPS have traditionally focused on the degradation of the photovoltaic array itself. This creates a significant gap by potentially overlooking the power electronic components, namely the converter and motor, which may, in fact, represent the primary bottleneck for system lifetime and the most critical focus for developing effective maintenance strategies.

This paper presents a state-of-the-art SSWPS for agricultural and rural use. The system is systematically modeled, including a solar photovoltaic array with an INC-based MPPT controller for maximum utilization of solar power. The system is modeled and simulated for different LUO converter duty cycles. At an optimal duty cycle of 0.75, simulation results demonstrate that the system achieves a maximum efficiency of 94.8%, with the BLDC motor reaching its rated speed of approximately 2065 rpm. Keeping this duty cycle, the Additionally, the current ripple is significantly reduced, and the stator Back Electromotive Force (BEMF) remains stable across operating conditions.

Further, the performance of the proposed system is investigated from different aspects as discussed in the following sections. , These outcomes confirm the system's robust performance and validate its effectiveness for reliable and energy-efficient water pumping in off-grid scenarios.

Main Contribution of Work

- This work presents a comprehensive and validated simulation framework that integrates four critical analysis domains: technical performance, long-term reliability, economic via- bility, and environmental impact (carbon savings). This provides a single, powerful tool for complete system evaluation.
- Identification of the optimal operating point, pinpointing a duty cycle of 0.75 as the point of maximum efficiency (94.78%).
- Computation of the high economic barrier precisely and contrast it with the compelling environmental benefits (annual carbon savings of 1,611 kg CO_2 and a 1.6-year carbon payback period).
- Analysis of a novel and significant finding about the system lifetime to identify power electronic components (the converter and motor) as the primary bottleneck for long-term reliability, showing that they degrade faster than the photovoltaic array. This insight redi- rects the focus to future maintenance and reliability improvements.
- Comparative analysis with the reported work to validate the technical efficacy of the proposed system.

Collectively, these contributions provide a robust and practical foundation for engineers, policymakers, and stakeholders to make more informed decisions about the design, deploy- ment, and operation of solar water pumping systems.

2 Proposed Methodology

This research employs a comprehensive simulation and computational methodology to analyze and optimize the proposed SSPWS. The methodology integrates theoretical modeling with simulation-based analysis to perform multi-criteria assessment. This provides holistic insights into the system to bridge the gap between academic research and practical implementation. The step-by-step procedure of the proposed work is illustrated in Figure 1. The primary step is to develop the framework of the system model. In this framework, individual subsystems are independently modeled and then integrated to capture the complex interactions of the system. The system is simulated under various operating conditions (such as at different duty cycles, solar irradiance, etc.) to assess its performance. In addition, this approach facilitates detailed component-level analysis while maintaining a system-level perspective, enabling identification of optimization opportunities that may not be apparent from isolated component studies. The analysis incorporates techno-economic, environmental impact, and long-term reliability assessment considering temporal variations, degradation effects, and

operational uncertainties to provide realistic performance projections over the system's operational lifetime as given in Section 4. In this way, the proposed work aims to validate existing research findings while providing enhanced analysis capabilities that support informed real-world deployment decisions.

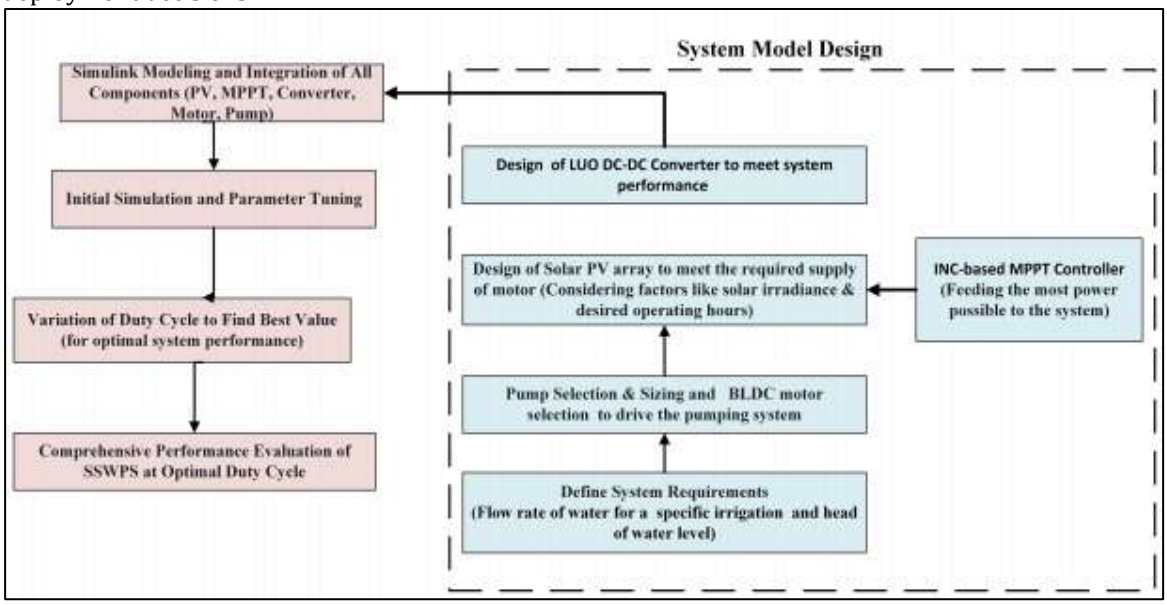


Figure 1: Proposed Methodology.

3 System Model Design

The SSPWPS system, shown in Figure 2, is developed through a detailed mathematical for- mulation at the component level, beginning with the definition of system requirements such as the desired flow rate for specific irrigation needs and the required head of water. Following this, the process moves to the selection and sizing of the centrifugal pump, along with the corresponding BLDC motor to drive the pumping system. Next, a Solar Photovoltaic (SPV) array is designed to meet the required power supply for the motor, considering factors such as solar irradiance and desired operating hours. To maximize power extraction under varying atmospheric conditions, an Incremental Conductance (INC) MPPT algorithm is implemented. This algorithm, via a pulse generator, controls the duty cycle of a LUO DC-DC converter. The selection of the LUO converter is justified by its widespread industrial adoption, which is due to its ability to provide a highly stable output voltage with minimal ripple, a critical factor for the reliable operation of sensitive loads [19]. Furthermore, the modeling of the LUO converter's dynamics is benchmarked against the reported work of [20] The system also fea- tures a closed-loop speed control mechanism where the actual motor speed is compared to a reference speed. The resulting error is fed to a PI controller, which works in conjunction with the MPPT to regulate the DC-DC converter's output voltage. This conditioned DC power is then supplied to a 3-phase inverter to converts it into the 3-phase AC power required to drive the BLDC motor. The motor's commutation is managed electronically using Hall sensor feedback; the sensor signals are processed to implement trapezoidal commutation logic, en

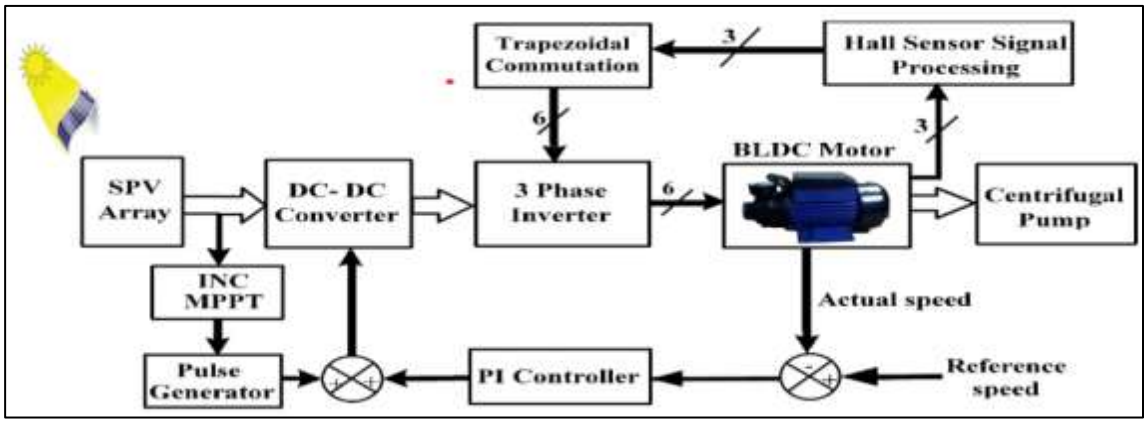


Figure 2: Block diagram of the proposed SSWPS.

suring proper sequencing of the inverter's power switches. Each subsystem is mathematically described and its parameters are detailed in Table 2 to analyze its behavior under various operating conditions. The proposed SSWPS modeling involves the comprehensive integration and analysis of its various components to ensure efficient and reliable operation.

3.1 Centrifugal Pump Design

Depending on the irrigation requirements and the head through which the water must be pumped, the first step is the pump design. The centrifugal pump used here is based on application requirements such as a 10-meter head, 50 L/minute discharge, which is a typical scenario of rural irrigation demand in India. The hydraulic power required by the pump is calculated using Equation 1, where ρ is the density of water, g is the acceleration due to gravity, Q is the flow rate, H is the head, and η is the efficiency of the pump.

$$P = \frac{\rho g Q H}{\eta} \approx 108.8\, W \qquad (1)$$

Here, ρ = 1000; kg/m3, g = 9.81m/s2, Q = 0.00083 m3/s, H = 10 m, η = 0.75.

The choice of the centrifugal pump is due to its capacity to achieve high efficiency. Such pumps are commonly utilized in low-head applications, especially indirect-drive solar-powered systems. The mechanism involves rotating impellers to generate sufficient pressure for lifting water by throwing it radially against a casing [21, 22]. The pump is directly coupled to the motor shaft, ensuring efficient mechanical energy transfer without the need for additional gearing or transmission. A key characteristic of centrifugal pumps is their need for a steady, non-pulsating torque to operate smoothly. The efficiency of centrifugal pumps is quite high, but decreases at lower speeds, which might be an issue for the solar water pumping system when solar irradiance levels are low. A 1.5 kW BLDC motor provides ample space to handle pump inefficiencies, startup surges, and variations in water levels.

3.2 BLDC Motor Modeling

The 1.5 kW, 230 V BLDC motor is modeled based on its electromagnetic, mechanical, and thermal characteristics. The fundamental relationship between the back electromotive force (E), motor speed (ω), and torque (T) is described by:

$$E = K_e \omega \qquad (2)$$

$$T = K_t I_q \qquad (3)$$

Where, K_e is the back EMF constant, K_t is the torque constant, and I_q is the quadrature-axis current, ω is the motor speed. The motor's efficiency (η_{motor}) is the ratio of mechanical output power to electrical input power [22]. The total losses ($P_{loss,motor}$) are the sum of copper losses (P_{Cu}), iron losses (P_{iron}), mechanical losses, and stray losses.

$$P_{Cu} = 3I^2 R_s \qquad (4)$$

$$P_{iron} = K_h \omega^{1.6} + K_h \omega^2 \qquad (5)$$

Where, R_s is the stator resistance per phase, and K_h and K_e are the ysteresis and eddy current loss coefficients.

3.3 Photovoltaic Array Modeling

The photovoltaic (PV) array is modelled based on a single-diode equivalent circuit, with parameters adjusted for real-world operating conditions. The model considers a 2-kW array composed of 250 W modules. To achieve this capacity, modules are arranged in $N_{series} = 4$ and $N_{parrallel} = 2$ configuration. The aggregate electrical characteristics of the array are determined by scaling the individual module specifications:

$$V_{oc} = V_{oc,module} \times N_{series} \quad (6)$$

$$I_{sc} = I_{sc,moodle} \times N_{parrallel} \quad (7)$$

$$V_{mpp} = V_{mpp,moodle} \times N_{series} \quad (8)$$

$$I_{mpp} = I_{mpp,moodle} \times N_{parrallel} \quad (9)$$

The model's output is corrected for environmental factors, including solar irradiance, G and ambient temperature, T. The corrected current, $I_{corrected}$ and voltage, $V_{corrected}$ are calculated as follows :

$$I_{corrected} = I_{mpp} \times \frac{G}{G_{STC}} \times \left(1 + K_i \left(\frac{T - T_{STC}}{T_{STC}}\right)\right) \quad (10)$$

$$V_{corrected} = V_{mpp} \times \left(1 + K_v \left(\frac{T - T_{STC}}{T_{STC}}\right)\right) \quad (11)$$

Where, G_{STC} and T_{STC} are the irradiance and temperature at Standard Test Conditions (STC), while K_i and K_v are the current and voltage temperature coefficients, respectively.

A degradation factor, D_{factor} applied over time t in years is presented below.

$$D_{factor} = \left(1 - \alpha_{deg}\right)^t \quad (12)$$

Where, $\alpha_{deg} = 0.5\%$ per annum (degradation rate) is considered. The Long-term performance is modeled using

$$P_{mpp} = V_{corrected} \times I_{corrected} \times D_{factor} \quad (13)$$

The incident solar irradiance is determined using standard solar geometry equations, which include solar declination (δ), hour angle (ω), and solar elevation (β). Finally, key performance metrics such as panel efficiency (η_{panel}) and fill factor (FF) are calculated as below:

$$\eta_{panel} = \frac{P_{mpp}}{G \times A_{panel}} \quad (14)$$

$$FF = \frac{P_{mpp}}{V_{oc,corrected} \times I_{sc,corrected}} \quad (15)$$

3.4 MPPT Controller Modeling

MPPT is achieved using the INC algorithm. This method tracks the MPPT by comparing the incremental conductance (dI/dV) with the instantaneous conductance (I/V). The condition for being at the MPPT is:

$$\frac{dI}{dV} = -\frac{I}{V} \; or \; \left(\frac{dP}{dV} = 0\right) \quad (16)$$

The algorithm adjusts the duty cycle (D) of the LUO converter to move the operating point towards the MPP based on the location on the P-V curve:

$$D_{new} = D_{old} \pm \Delta D_{step} \quad (17)$$

Where, the sign of the step (ΔD_{step}) depends on the sign of dP/dV. The performance of the MPPT controller is quantified by its tracking efficiency ($\eta_{tracking}$) and convergence time (t_{conv}).

$$\eta_{tracking} = \frac{\int P_{actual}(t)dt}{\int P_{mpp,theortical}(t)dt} \times 100\% \quad (18)$$

$$t_{conv} = Time\ to\ reach\ and\ settle\ within\ 95\%\ of\ P_{mpp,theortical} \quad (19)$$

3.5 LUO DC-DC Converter Modeling

The positive output LUO converter serves as the interface between the PV array and the inverter. Its primary function is to boost the PV voltage while tracking the maximum power point. The ideal voltage gain (M) of the converter is a function of the duty cycle (D):

$$M = \frac{V_{out}}{V_{in}} = \frac{D}{1-D} \quad (20)$$

($L_{1,cir}, L_{2,cir}$) required to ensure CCM are given below:

$$L_{1,cir} = \frac{(1-D)^2 R_{load}}{2f_s} \quad (21)$$

$$L_{2,cir} = \frac{D(1-D)R_{load}}{2f_s} \quad (22)$$

Where, R_{load} is the load resistance and f_s is the switching frequency. The voltage ripple across the capacitors ($\Delta V_{c1}, \Delta V_{c2}$) is determined by:

$$\Delta V_{c1} = \frac{I_{out}D}{f_s C_1} \quad (23)$$

$$\Delta V_{c2} = \frac{I_{out}(1-D)}{f_s C_2} \quad (24)$$

A comprehensive loss model is used to calculate the converter's efficiency (η_{conv}) [31-32]. The total power loss (P_{loss}) includes conduction losses (P_{cond}), switching losses (P_{sw}), and losses in the passive components (P_L , P_c).

$$P_{loss} = P_{cond} + P_{sw} + P_L + P_c \quad (25)$$

Finally, thermal analysis is performed to assess component stress. The junction temperature (T_j) is estimated based on the total power loss and the junction-to-ambient thermal resistance (θ_{ja}):

$$T_j = T_{ambient} + P_{loss} \times \theta_{ja} \quad (26)$$

Parameter	Value	Description
PV Array Configuration		
Rated Power	2000 W	Total array capacity
Module Configuration	4S × 2P	4 series, 2 parallel
Individual Module Power	250 W	Single module rating
LUODC-DC Converter Parameter		
Primary Inductor (L1)	6.6 mH	Main energy storage inductor
Secondary Inductor (L2)	3.3 mH	Output filter inductor
Input Capacitor (C1)	21.7 µF	Input voltage smoothing
Output Capacitor (C_2)	18.9 μF	Output voltage filtering
Switching Frequency (f_s)	20 kHz	MOSFET switching rate
BLDC Motor Specifications		
Rated Power	1500 W	Motor power rating
Rated Voltage	230 V	DC Bus Voltage
Rated Speed	2065 RPM	Nominal rotational speed
Number of Poles	4	Magnetic pole pairs
MPPT Controller Configuration		
Algorithm Type	InC	Incremental Conductance
Step Size	0.01	Duty cycle adjustment
Minimum Duty Cycle	0.1	Lower operating point
Maximum Duty Cycle	0.9	Upper operating point
Voltage Threshold	0.1 V	Minimum voltage change

4 Simulations

A simulation model of the SSPWPS system is created by integrating mathematical models of the required subsystems including PV array, LUO converter, BLDC motor, and MPPT controller. Using the specific parameters detailed in Table 2, a comprehensive simulation is conducted to validate the system's performance across diverse operating conditions. These simulation parameters are derived directly from the component models and standard application requirements. The key parameters include a switching frequency (fs) of 20 kHz for the LUO converter, an MPPT controller step size (ΔD) of 0.01, and PI controller gains (K_P and K_I) tuned for stable speed regulation. To accurately capture the high-frequency dynamics of the system, the simulation time step is set to 10 µs that will ensure numerical stability. Firstly, the system is simulated under standard test conditions with an irradiance of 1000 W/m2 and a temperature of 250C. This scenario establishes a performance baseline, validating the PV array's power output and the steady-state efficiency of the LUO converter and BLDC motor at their nominal operating points. Then, a realistic daily operation is simulated using a full-day irradiance profile, modelled as a bell-shaped curve for the system power produced along with the corresponding water flow rate (refer to Figure 3) peaking at solar noon. This dynamic test is crucial for assessing the real-world effectiveness of the INC-MPPT algorithm, including its tracking accuracy and response time

under continuously changing solar input. This enables us to completely analyse the converter and motor performance over an operational cycle.
The results obtained from these experiments provide a comprehensive validation of the proposed system model. These findings are presented and discussed in the following section.

5 Performance Analysis

This section presents the quantitative findings from the simulations, corresponding to the key performance indicators defined in the methodology. The data is first presented for the optimal operating point under Standard Test Conditions (STC), followed by a detailed analysis across various operating conditions and time horizons.

(i) System Performance under STC

This section presents the quantitative findings from the simulations. The individual efficiencies of the LUO converter (ηconv) and the BLDC motor (ηmotor) are plotted as a function of input power to identify performance across the operating range. The data is first presented for the optimal operating point, followed by a detailed analysis across various operating conditions and time horizons. The simulation results under STC indicate a peak overall efficiency of 94.78% when the system operatedata duty cycle of 0.75 (Figure 4). At this operating point, the system successfully achieved the rated motor speed of 2065 RPM and delivered a peak torque of 5.0 Nm. The current ripple was measured to be 0.3 A . A summary of the system's peak performance metrics is provided in Table 3.

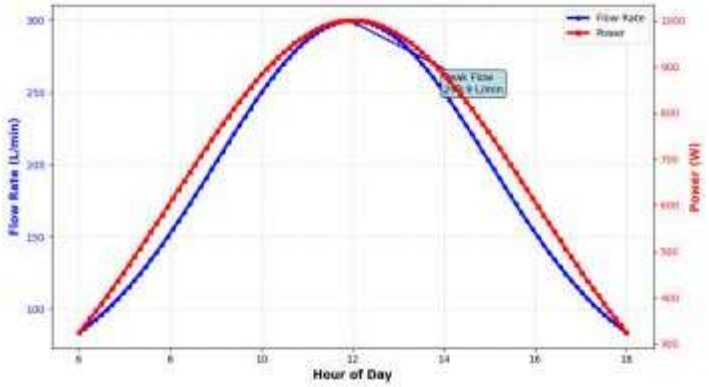


Figure 3: Daily Power Profile (Summer)

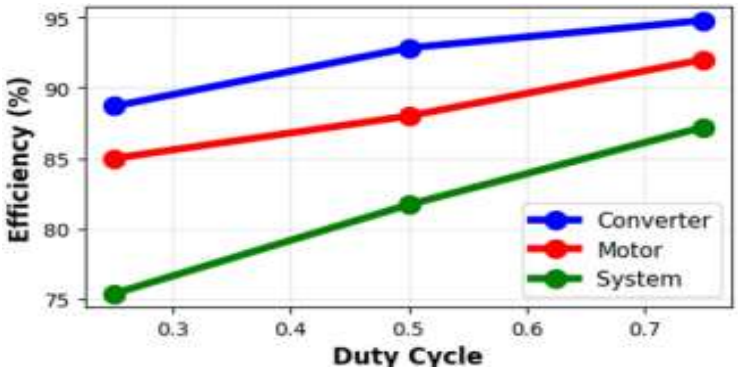


Figure 4: System Efficiency Analysis

Table 3: System Performance Summary at Optimal Operating Point (D=0.75)

Parameter	Value	Unit
Maximum System Efficiency	94.78	%
Rated Motor Speed Achieved	2065	RPM
Peak Torque Output	5.0	Nm
Minimum Current Ripple	0.3	A

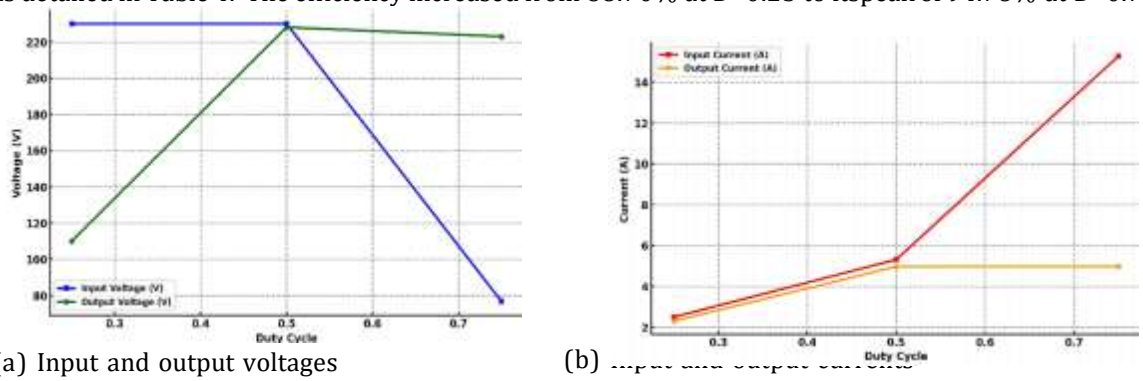
(ii) Component Performance

The performance of the system's key components was evaluated across a range of duty cycles to understand their behavior under varying power input levels, simulating conditions from high to low solar irradiance.

(a) LUO Converter Performance

The performance of LUO Converter is fundamental to the system's success, demonstrating exceptional voltage regulation and high-gain capability. As detailed in Table 4 and illustrated in Figure 5, the converter maintains a stable output voltage crucial for the motor. The most significant finding occurs at a duty cycle of D=0.75, which simulates low irradiance conditions. Despite the input voltage dropping to just 76.67 V, the converter successfully boosts and regulates the output to a stable 223.0 V. This high-gain performance, achieved while drawing a higher input current to maintain power transfer, validates the converter's

critical role in ensuring uninterrupted motor operation under fluctuating solar conditions. The efficiency and thermal characteristics of the LUO converter vary significantly with the duty cycle, as detailed in Table 4. The efficiency increased from 88.70% at D=0.25 to itspeak of 94.78% at D=0.75.



(a) Input and output voltages (b)

Figure 5: Voltage and current characteristics of the LUO converter across duty cycles.

Table 4: LUO converter electrical prformance

D	V_1(V)	V_2(V)	I_1(A)	I_2(A)	η (%)
0.25	230	110	2.5	2.3	88.70
0.50	230	228.1	5.311	4.972	92.84
0.75	76.67	223.0	15.27	4.976	94.78
0.25	230	110	2.5	2.3	88.70

(b) MPPT Controller Performance

The performance of the INC-MPPT controller is presented in Table 5, demonstrating its effectiveness in achieving close to optimal power tracking and stable system operation. The tracking efficiency (ηtracking) is calculated by comparing the actual power extracted from the PV array against the theoretical maximum available power throughout the day. The convergence time (tconv) and steady-state error are also measured. The results are shown in Table 5. The tracking efficiency (ηtracking) is calculated by comparing the actual power extracted from the PV array against the theoretical maximum available power throughout the day. The convergence time (tconv) and steady-state error are also measured.

(c) BLDC Motor and Pump Performance

The stability provided by the LUO converter directly translates to improved performance in the BLDC motor. Performance quality metrics, including current ripple (ΔI), torque ripple (ΔT), and Total Harmonic Distortion (THD) of the current, are evaluated to assess the drive quality:

$$T = K_t \Delta I \quad (27)$$

$$THD = \frac{\sqrt{\sum I_h^2}}{I_{fundamental}} \times 100\% \quad (28)$$

$$T_j = T_{jambient} + P_{loss} \times \theta_{ja} \quad (29)$$

$$\Delta I = \frac{V_{dc} \times D \times (1-D)}{L_s \times f_s} \quad (30)$$

$$E = \frac{K_e \times \omega \times N_{pole}}{2} \quad (31)$$

where, $K_e = 0.995\, Vs/rad$ (back EMF constant), $K_e = 0.38\, Nm/A$ (torque constant), ω = angular velocity (rad/s), I_{eq}= quadrature current (A), $N_{pole} = 4$ (number of poles), T_j is junction temperature in °C. As shown in Table 6, motor speed, torque, and power quality improve as the duty cycle increases towards the optimal point. At D=0.75, the motor achieves its rated speed of 2065 RPM and a peak torque of 5.0 Nm. Critically, the current ripple is minimized to 0.3 A, a significant reduction from 0.8 A at the lower duty cycle, indicating much smoother and more efficient operation. The corresponding increase in back-EMF confirms proper motor excitation.

Head (m)	D=0.25	D=0.5	D=0.75
6	24	32	38
8	22	30	36
10	20	28	34
12	18	26	32
14	16	24	30

Table 5: Performance Metrics of the INC MPPT Controller.

Parameter	Value
Settling time	8 sec
Minimum Current Ripple	168 %
Tracking Error (RMS)	12.6 %
Average Computation Time	0.36 sec

Table 6: BLDC Motor Performance vs. Duty Cycle.

D	N	T	η	$I_{ripples}$	T_j	Back EMF
0.25	1850 RPM	4.0 Nm	85%	0.8 A	59^0C	150V
0.5	1990 RPM	4.8 Nm	88%	0.5A	66.6^0C	210V
0.75	2065RPM	5.0 Nm	92%	0.3A	68.8^0C	203V

(iii) Annual and Seasonal Performance

With the optimal duty cycle established at 0.75, the system's dynamic performance was subsequently evaluated under various operating conditions. The simulation projected a total annual energy production of 1,895.8 kWh, resulting in 52,178,138 L of pumped water (Table 8). Furthermore, the simulation investigated the impact of seasonal variation on the system's output, as detailed in Table 9. This table presents the seasonal energy output, water output, and Capacity Factor (CF) for the four seasons: winter, spring, autumn, and summer.

$$E_{annual} = \left(E_{daily\ season} \times Day_{season}\right) \quad (32)$$

$$CF = \frac{E_{annual}}{P_{rated} \times 8760} \quad (33)$$

n

The average system CF is calculated to be 11.4%. Performance varied seasonally, with summer months yielding 8.4 kWh and winter months producing 2.6 kWh. This seasonal variation can be seen in Figure 6.

Table 8: Annual Performance Projection

Parameter	Value

Annual Production	1,895.8 kWh
Annual Water Pumping	52, 178, 138 L
Annual Daily Water	1, 42, 956 L/day
System Efficiency	94.8%

Table 9: Seasonal Performance Variation

Season	Energy Production (kWh/day)	Water Output (L/day)	Capacity Factor (%)
Winter	2.6	71478	8.5
Springer	5.2	142956	12.1
Summer	8.4	266568	15.5
Autumn	4.6	231226	9.5

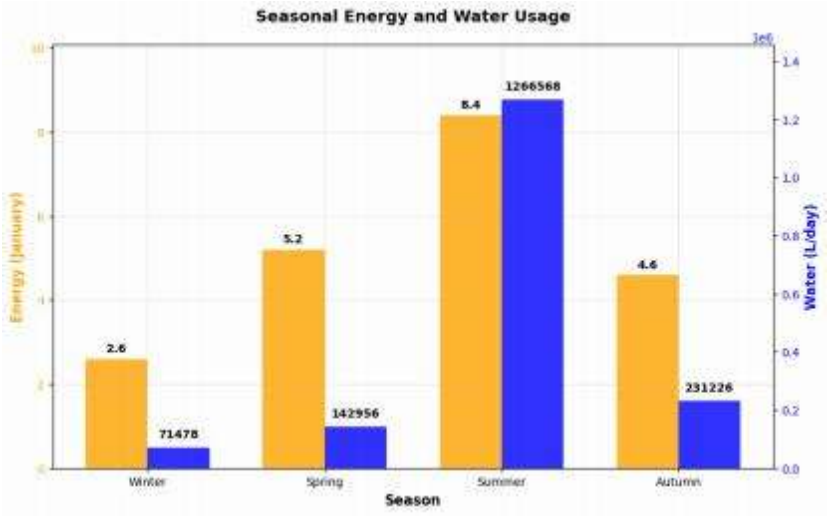


Figure 6: Seasonal Performance Variation

(iv) Economic and Environmental Metrics

To carryout this analysis, it is assumed that the initial capital cost of the system is 8,000 USD, and maintenance cost per annum to be 200 USD.

The LCOE of this system is computed as \$0.351/kWh (Table 10). The mathematical formu- lation for LCOE is given by:

$$LCOE = \frac{I_0 + \sum \frac{M_t + F_t}{(1+r)^t}}{\sum \frac{E_t}{(1+r)^t}} \quad (34)$$

Environmentally, the system is projected to save 1,611 kg of CO2 annually, leading to a carbon payback period of 1.6 years. These metrics were found using:

$$Payback\ Period = \frac{I_0}{CF_{annual}} \quad (35)$$

$$\text{Annual saving} = \text{Annual energy (kWh)} \times \text{Electricity rate} - \text{Maintenance cost} \quad (36)$$

$$Carbon\ Payback = \frac{System\ Embodied\ Carbon}{Annual\ Carbon\ Savings}$$

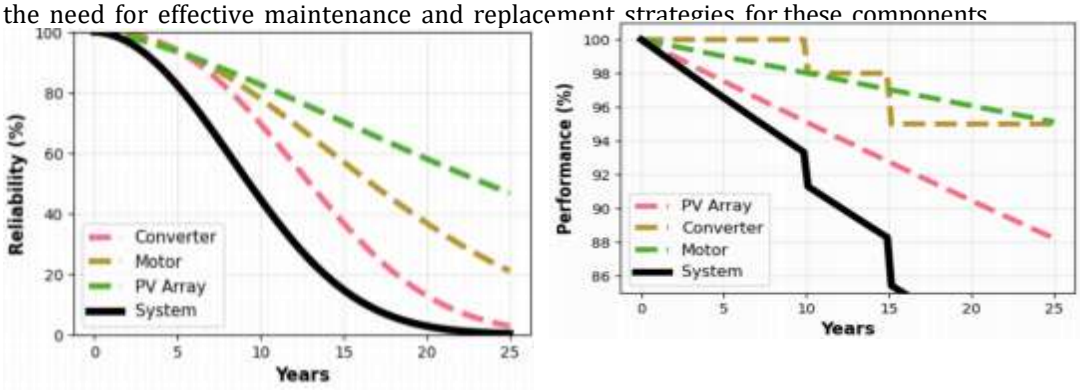
Where, $Annual\ Carbon\ Savings = Annual\ Energy \times Grid\ Emission\ Factor$

Table 10: Economic Analysis

Parameter	Value
LCOE	0.351 \$/kWh
Simple Payback Period	0.63 years
Net Present Value (25 years)	1,53,644 \$

(v) Long-Term Reliability Projection

The expression for reliability is given below. Figure 7a and 7b shows the long-term perfor- mance degradation and system reliability analysis projection of the system over 25 years. The reliability of the converter, motor, and PV array is plotted, with the system'soverall reliability (black curve) showing a significant degradation to 60% of its initial capacity by the end of the 25 years. The PV array maintains better durability, while the converter and motor degrade more quickly, highlighting the need for effective maintenance and replacement strategies for these components.



(a) Long-term Performance Degration (b) System Reliability Analysis

Figure 7: Long-term Reliability and Performance Projection.

5.1 Key Findings and Implications

Based on the preceding analysis, several key findings and implications emerge regarding the system's performance, viability, and operational constraints:

1. Optimal operating strategy is critical: The performance of the system is highly depen- dent on the duty cycle of the converter. An operating point of D=0.75 is unequivo- cally the optimal strategy, as it simultaneously produces the highest system efficiency (94.78%), maximizes motor output, and ensures the lowest thermal stress on electronic components.
2. High technical performance within strict boundaries: At its optimal point, the system shows excellent technical capabilities by achieving its rated speed (2065 RPM) and delivering a high torque (5.0 Nm). The model's prediction of extreme temperatures under these conditions establishes a clear operational boundary to prevent component failure.

3. Economic viability is application-dependent: Despite its technical strengths, the system faces significant economic hurdles. A high LCOE ($0.351/kWh) and a negative NPV indicate that it is not economically competitive with conventional grid power. Its fi- nancial viability is therefore confined to off-grid applications where it displaces more expensive energy sources, such as diesel generators.
4. The primary justification is environmental. The strongest value proposition of the sys- tem is environmental, with annual carbon savings of 1,611 kg of CO_2 . A rapid carbon payback period of only 1.6 years, it offers a compelling pathway to decarbonize off-grid water pumping, providing immediate and long-lasting environmental benefits.
5. Power electronics dictate long-term reliability: The performance of the system is pro- jected to degrade to 60% of its initial capacity over a 25-year life. Critically, the analysis identifies power electronics (converter and motor) as the primary drivers of this degra- dation, not the more durable photovoltaic array. This insight is crucial for developing effective long-term maintenance and replacement strategies to ensure the longevity of the system.

6 Comparative Analysis

Table 11 provides a comprehensive comparison of key performance at STC parameters, in- cluding speed, torque, efficiency, current ripple, converter type, and MPPT technique, across four different schemes. The proposed scheme, featuring a LUO DC-DC converter and Incre- mental Conductance (INC) MPPT technique, outperforms the existing techniques in terms of efficiency (94.78%), current ripple (0.3 A), and per-day water drawing capacity. The compara- tive analysis highlights significant improvements in torque and speed, indicating the enhanced potential of the proposed scheme for practical applications. Furthermore, the adoption of the LUO DC-DC converter offers better

performance stability over conventional boost converters, making it a promising solution for high-efficiency systems.

Table 11: Comparative Analysis for Performance Parameters at STC.

Parameter	**Proposed Scheme**	**[10]**	**[23]**	**[14]**
Speed (RPM)	2065	2000	2100	1950–2020
Torque (Nm)	5.0	4.6	5.1	4.2–4.9
Efficiency (%)	94.78	85–89	89–91	82–90
Current Ripple (A)	0.3	0.4–0.7	~0.4	–
Converter Type	LUO DC–DC	Conventional Boost	LUO DC–DC	Interleaved Boost
MPPT Technique	INC	Adaptive PI	None (direct control)	P&O + ANN Hybrid

7 Conclusion

This research work presented a comprehensive simulation model for a solar-powered water pumping system featuring a LUO converter and a BLDC motor. The research successfully demonstrated the system's technical viability, particularly when operated under an optimal duty cycle of 0.75, where it achieved a peak efficiency of 94.78%. The analysis revealed a critical operational insight: while the system is highly efficient at its nominal operating point, its performance and component reliability are severely compromised at lower duty cycles due to thermal stress. From an economic standpoint, the system is not a viable replacement for grid-connected applications but presents a strong value proposition for off-grid scenarios. This is especially true when considering its significant environmental benefits, including a rapid 1.6-year carbon payback period. Ultimately, this work provides a detailed framework for analyzing and optimizing SSPWPS designs, and underscores the critical importance of integrated component analysis for achieving both high efficiency and long-term reliability. A key limitation of this research is its reliance on a conventional Incremental Conductance MPPT algorithm. Therefore, future work will focus on a comparative analysis with advanced intelligent controllers, such as those based on fuzzy logic or artificial neural networks. This investigation will aim to quantify potential improvements in tracking efficiency and system responsiveness, particularly under rapidly changing atmospheric conditions.

Authors Disclosure of Interest

The authors have no conflict of interest to declare.

Contribution of Each Author

Conception: U.K.J., R.G., N.N.; Design: U.K.J.; Supervision:R.G., N.N.; Material: U.K.J.; Data Collection-and/or Processing:U.K.J.; Analysis and/or Interpretation: U.K.J., R.G., N.N.; Literature Review:U.K.J., R.G., N.N.; Writing-: U.K.J.; Critical Review:U.K.J., R.G., N.N.

Funding

The authors declared that this research work has not received financial support.

References

[1] International Energy Agency (IEA), "World electricity final consumption by sector, 1974–2019," IEA. [Online]. Available: https://www.iea.org/data-and-statistics/charts/world-electricity-final-consumption-by-sector-1974-2019.

[2] Statista Research Department, "Global electricity consumption 1980–2021," Statista, 2023. [Online]. Available: https://www.statista.com/statistics/280704/world-power-consumption

[3] A. Al-Badi, H. Yousef, T. Al Mahmoudi, M. Al-Shammaki, A. Al-Abri, and A. Al Hinai, "Sizing and modelling of photovoltaic water pumping system," Int. J. Sustain. Energy, vol. 37, no. 5, pp. 415–427, 2018.

[4] M. Gasque et al., "Energy efficiency optimization in Battery-Based photovoltaic pump-ing schemes," IEEE Access, vol. 10, pp. 54064–54078, Jan. 2022, doi: 10.1109/ac-cess.2022.3175586.

[5] P. Fairley, "Off-grid solar's killer app: Solar pumps, batteries, and microcredit are trig-gering an African agricultural renaissance," IEEE Spectr., vol. 58, no. 6, pp. 44–49, 2021.

[6] J. S. Rajesh, R. Karthikeyan, and R. Revathi, "Analysis and control of grid-interactive PV-fed BLDC water pumping system with optimized MPPT for DC-DC converter," Sci. Rep., vol. 14, p. 25963, 2024.
[7] A. Mahjoubi, R. F. Mechlouch, B. Mahdhaoui, and A. Ben Brahim, "Techno-economic analysis and modelling of a remote photovoltaic water pumping system in the desert of Tunisia," Int. J. Sustain. Energy, vol. 32, no. 5, pp. 434–448, 2013, doi: 10.1080/14786451.2013.831417.
[8] T. R. Ayodele, A. S. O. Ogunjuyigbe, and O. A. Adeniran, "Evaluation of solar powered water pumping system: the case study of three selected abattoirs in Ibadan, Nigeria," Int. J. Sustain. Eng., vol. 12, no. 1, pp. 58–69, 2019.
[9] S. Angadi, U. R. Yaragatti, Y. Suresh, and A. B. Raju, "Comprehensive review on solar, wind and hybrid wind- PV water pumping systems— An electrical engineering perspec- tive," CPSS Trans. Power Electron. Appl., vol. 6, no. 1, pp. 1–19, Mar. 2021.
[10] A. K. Mishra, B. Singh, and T. Kim, "An efficient and credible grid-interfaced solar PV water pumping system with energy storage," IEEE J. Photovolt., vol. 12, no. 3, pp. 880–887, 2022, doi: 10.1109/JPHOTOV.2022.3161281.
[11] H. Parveen and B. Singh, PV Fed synchronous reluctance mo- tor driven water pumping system with grid integration and seam- less operability. 2022. doi: 10.1109/piicon56320.2022.10045176. Available: https://doi.org/10.1109/piicon56320.2022.10045176
[12] S. Jeyanthi and M. B. Veerayan, "Performance analysis of a quasi-Z-source converter for solar photovoltaic system powered water pumping system," Electr. Power Compon. Syst., vol. 52, no. 1, pp. 1–19, 2024.
[13] C. Mokhtara, B. Negrou, B. Settou, and M. M. Samy, "Design optimization of off-grid hybrid renewable energy systems considering the effects of building energy performance and climate change: Case study of Algeria," Energy, vol. 219, p. 119605, 2021, doi: 10.1016/j.energy.2021.119605.
[14] S. Habib, H. Liu, M. Tamoor, M. A. Zaka, Y. Jia, A. G. Hussien, H. M. Zawbaa, and K. Salah, "Technical modelling of solar photovoltaic water pumping system and evaluation of system performance and their socio-economic impact," Sol. Energy, vol. 258, pp. 193–207, 2023, doi: 10.1016/j.solener.2023.01.057.
[15] M. M. A. Awan, M. Y. Javed, A. B. Asghar, and K. Ejsmont, "Performance optimization of a ten check MPPT algorithm for an off-grid solar photovoltaic system," Energies, vol. 15, no. 6, p. 2104, 2022.
[16] L. Cao, S. Wang, J. Zhu, X. Wang, and W. Hu, "Life cycle assessment of solar PV water pumping system for carbon emissions reduction at a location: a case study," Energy Sources, Part A: Recovery, Utilization, and Environmental Effects, vol. 46, no. 1, pp. 4704–4717, 2024.
[17] J. Yang, A. Olsson, J. Yan, and B. Chen, "A hybrid life-cycle assessment of CO2 emissions of a PV water pumping system in China," Energy Procedia, vol. 61, pp. 2871–2875, 2014.
[18] R. V. Vamja and M. A. Mulla, "Standalone solar water pumping system utilizing parallel connected quadratic boost converter: controller design and hardware in loop implemen- tation," Energy Sources, Part A: Recovery, Utilization, and Environmental Effects, vol. 47, no. 1, pp. 1159–1175, 2025.
[19] M. Aberoumandazar and F. M. Shahir, "Stability analysis of LUO converter using state space modeling," Journal of Circuits Systems and Computers, vol. 30, no. 07, p. 2150127, Nov. 2020, doi: 10.1142/s0218126621501279.
[20] D. N. Jayachandran, V. Krishnaswamy, L. Anbazhagan, and K. Dhandapani, "Modelling and analysis of voltage mode controlled Luo converter," Amer. J. Appl. Sci., vol. 12, no. 5, pp. 766–774, 2015.
[21] W. V. Jones, "Motor selection made easy: Choosing the right motor for centrifugal pump applications," IEEE Ind. Appl. Mag., vol. 19, no. 6, pp. 36–45, 2013.
[22] M. Volk, Pump Characteristics and Applications, 3rd ed. Boca Raton, FL, USA: CRC Press, Taylor & Francis Group, 2014.
[23] G. A. Thirupalu and S. Sridhar, "Solar PV array fed with Luo converter and hysteresis- control three-phase inverter of BLDC motor driven water pump," NeuroQuantology, vol. 20, no. 20, pp. 1687–1692, 2022.
[24] Z. Al-Omari, N. Khlaifat, and M. Haddad, A feasibility study of combining solar/wind energy to power a water pumping system in Jordan's Desert/Al-Mudawwara village," Environ. Sustain. Indicators, vol. 25, p. 100555, 2025.

[25] A. Goswami, M. Sreejeth, and M. Singh, "Investigation and mitigation of unbalanced hall sensor signal faults in sensored brushless DC motor drives," Electr. Eng., 2024, doi: 10.1007/s00202-024-02245-7.
[26] A. Goswami, M. Sreejeth, and M. Singh, "DC link current-based commutation delay compensation method for sensored brushless DC motor drives," J. Power Electron., 2024, doi: 10.1007/s43236-024-00781-w.
[27] S. Habib, H. Liu, M. Tamoor, M. A. Zaka, Y. Jia, A. G. Hussien, H. M. Zawbaa, and S. Kamel, "Technical modelling of solar photovoltaic water pumping system and evaluation of system performance and their socio-economic impact," Heliyon, vol. 9,no. 5,p. e16105, 2023, doi: 10.1016/j.heliyon.2023.e16105.
[28] N. Abu-Hamdeh and K. Alnefaie, Techno-economic comparison of solar power tower system/photovoltaic system/wind turbine/diesel generator in supplying electrical energy to small loads," J. Taibah Univ. Sci., vol. 13, no. 1, pp. 216–224, 2019.